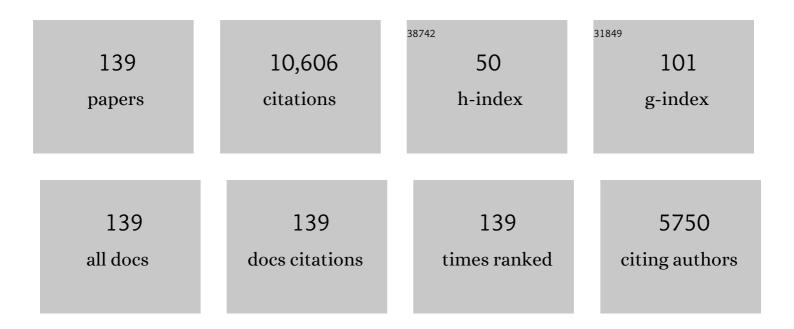
Andres Cuevas

List of Publications by Year in descending order

Source: https://exaly.com/author-pdf/11818869/publications.pdf Version: 2024-02-01



#	Article	IF	CITATIONS
1	Silicon solar cells with passivating contacts: Classification and performance. Progress in Photovoltaics: Research and Applications, 2023, 31, 310-326.	8.1	12
2	Morphology, microstructure, and doping behaviour: A comparison between different deposition methods for poly‣i/SiO _{<i>x</i>} passivating contacts. Progress in Photovoltaics: Research and Applications, 2021, 29, 857-868.	8.1	16
3	Polysilicon passivated junctions: The next technology for silicon solar cells?. Joule, 2021, 5, 811-828.	24.0	88
4	Investigation of Gallium–Boron Spinâ€On Codoping for poly‣i/SiO _{<i>x</i>} Passivating Contacts. Solar Rrl, 2021, 5, 2100653.	5.8	3
5	Investigation of Gallium–Boron Spinâ€On Codoping for poly‣i/SiO _{<i>x</i>} Passivating Contacts. Solar Rrl, 2021, 5, .	5.8	1
6	Hydrogenation Mechanisms of Poly‣i/SiO _{<i>x</i>} Passivating Contacts by Different Capping Layers. Solar Rrl, 2020, 4, 1900476.	5.8	13
7	Hydrogenation Mechanisms of Poly‧i/SiO _{<i>x</i>} Passivating Contacts by Different Capping Layers. Solar Rrl, 2020, 4, 2070033.	5.8	10
8	Influence of PECVD Deposition Power and Pressure on Phosphorus-Doped Polysilicon Passivating Contacts. IEEE Journal of Photovoltaics, 2020, 10, 1239-1245.	2.5	6
9	Dual-Function Electron-Conductive, Hole-Blocking Titanium Nitride Contacts for Efficient Silicon Solar Cells. Joule, 2019, 3, 1314-1327.	24.0	91
10	Hydrogenation of polycrystalline silicon films for passivating contacts solar cells. , 2019, , .		2
11	Electron-Conductive, Hole-Blocking Contact for Silicon Solar Cells. , 2019, , .		0
12	Hydrogen-Assisted Defect Engineering of Doped Poly-Si Films for Passivating Contact Solar Cells. ACS Applied Energy Materials, 2019, 2, 8783-8791.	5.1	12
13	High efficiency n-type silicon solar cells with passivating contacts based on PECVD silicon films doped by phosphorus diffusion. Solar Energy Materials and Solar Cells, 2019, 193, 80-84.	6.2	72
14	Dopantâ€Free Partial Rear Contacts Enabling 23% Silicon Solar Cells. Advanced Energy Materials, 2019, 9, 1803367.	19.5	77
15	Tantalum Nitride Electronâ€Selective Contact for Crystalline Silicon Solar Cells. Advanced Energy Materials, 2018, 8, 1800608.	19.5	112
16	Direct Observation of the Impurity Gettering Layers in Polysilicon-Based Passivating Contacts for Silicon Solar Cells. ACS Applied Energy Materials, 2018, 1, 2275-2282.	5.1	22
17	Laserâ€Patterned nâ€Type Frontâ€Junction Silicon Solar Cell With Tantalum Oxide/Silicon Nitride Passivation and Antireflection. Solar Rrl, 2018, 2, 1700187.	5.8	3
18	Stable Dopant-Free Asymmetric Heterocontact Silicon Solar Cells with Efficiencies above 20%. ACS Energy Letters, 2018, 3, 508-513.	17.4	164

#	Article	IF	CITATIONS
19	Effective impurity gettering by phosphorus- and boron-diffused polysilicon passivating contacts for silicon solar cells. Solar Energy Materials and Solar Cells, 2018, 179, 136-141.	6.2	46
20	Carrier population control and surface passivation in solar cells. Solar Energy Materials and Solar Cells, 2018, 184, 38-47.	6.2	109
21	Tantalum Oxide Electron-Selective Heterocontacts for Silicon Photovoltaics and Photoelectrochemical Water Reduction. ACS Energy Letters, 2018, 3, 125-131.	17.4	127
22	Tantalum Nitride Hole-Blocking Layer for Efficient Silicon Solar Cells. , 2018, , .		0
23	Impurity Gettering by Diffusion-doped Polysilicon Passivating Contacts for Silicon Solar Cells. , 2018, ,		2
24	23% efficient n-type crystalline silicon solar cells with passivated partial rear contacts. , 2018, , .		1
25	Sub-Bandgap Luminescence from Doped Polycrystalline and Amorphous Silicon Films and Its Application to Understanding Passivating-Contact Solar Cells. ACS Applied Energy Materials, 2018, 1, 6619-6625.	5.1	18
26	Temperature and Humidity Stable Alkali/Alkalineâ€Earth Metal Carbonates as Electron Heterocontacts for Silicon Photovoltaics. Advanced Energy Materials, 2018, 8, 1800743.	19.5	35
27	Zirconium oxide surface passivation of crystalline silicon. Applied Physics Letters, 2018, 112, .	3.3	19
28	23% efficient p-type crystalline silicon solar cells with hole-selective passivating contacts based on physical vapor deposition of doped silicon films. Applied Physics Letters, 2018, 113, .	3.3	84
29	Characterization and Diagnosis of Silicon Wafers, Ingots, and Solar Cells. , 2018, , 1119-1154.		5
30	A Low Resistance Calcium/Reduced Titania Passivated Contact for High Efficiency Crystalline Silicon Solar Cells. Advanced Energy Materials, 2017, 7, 1602606.	19.5	97
31	Highly effective electronic passivation of silicon surfaces by atomic layer deposited hafnium oxide. Applied Physics Letters, 2017, 110, .	3.3	58
32	Passivation of Phosphorus Diffused Black Multi rystalline Silicon by Hafnium Oxide. Physica Status Solidi - Rapid Research Letters, 2017, 11, 1700296.	2.4	5
33	Microchannel contacting of crystalline silicon solar cells. Scientific Reports, 2017, 7, 9085.	3.3	8
34	Calcium contacts to nâ€ŧype crystalline silicon solar cells. Progress in Photovoltaics: Research and Applications, 2017, 25, 636-644.	8.1	60
35	Conductive and Stable Magnesium Oxide Electronâ€ S elective Contacts for Efficient Silicon Solar Cells. Advanced Energy Materials, 2017, 7, 1601863.	19.5	174
36	Efficient electron contacts for \$n\$-type silicon solar cells using Magnesium metal, oxide, and fluoride. , 2017, , .		0

3

#	Article	IF	CITATIONS
37	Silicon Surface Passivation by Gallium Oxide Capped With Silicon Nitride. IEEE Journal of Photovoltaics, 2016, 6, 900-905.	2.5	18
38	Low resistance Ohmic contact to p-type crystalline silicon via nitrogen-doped copper oxide films. Applied Physics Letters, 2016, 109, .	3.3	21
39	Characterisation of sputtering deposited amorphous silicon films for silicon heterojunction solar cells. , 2016, , .		1
40	Survey of dopant-free carrier-selective contacts for silicon solar cells. , 2016, , .		12
41	A magnesium/amorphous silicon passivating contact for <i>n</i> -type crystalline silicon solar cells. Applied Physics Letters, 2016, 109, .	3.3	44
42	Magnesium fluoride based electron-selective contact. , 2016, , .		0
43	Passivating contacts for silicon solar cells based on boron-diffused recrystallized amorphous silicon and thin dielectric interlayers. Solar Energy Materials and Solar Cells, 2016, 152, 73-79.	6.2	81
44	Superacid Passivation of Crystalline Silicon Surfaces. ACS Applied Materials & Interfaces, 2016, 8, 24205-24211.	8.0	38
45	Efficient silicon solar cells with dopant-free asymmetric heterocontacts. Nature Energy, 2016, 1, .	39.5	461
46	Titanium oxide: A re-emerging optical and passivating material for silicon solar cells. Solar Energy Materials and Solar Cells, 2016, 158, 115-121.	6.2	67
47	Magnesium Fluoride Electron-Selective Contacts for Crystalline Silicon Solar Cells. ACS Applied Materials & Interfaces, 2016, 8, 14671-14677.	8.0	188
48	Lithium Fluoride Based Electron Contacts for High Efficiency nâ€Type Crystalline Silicon Solar Cells. Advanced Energy Materials, 2016, 6, 1600241.	19.5	134
49	High-efficiency crystalline silicon solar cells: status and perspectives. Energy and Environmental Science, 2016, 9, 1552-1576.	30.8	790
50	Passivation of c-Si surfaces by sub-nm amorphous silicon capped with silicon nitride. Applied Physics Letters, 2015, 107, .	3.3	9
51	Plasma enhanced atomic layer deposition of gallium oxide on crystalline silicon: demonstration of surface passivation and negative interfacial charge. Physica Status Solidi - Rapid Research Letters, 2015, 9, 220-224.	2.4	35
52	Silicon nitride/silicon oxide interlayers for solar cell passivating contacts based on PECVD amorphous silicon. Physica Status Solidi - Rapid Research Letters, 2015, 9, 617-621.	2.4	15
53	Recombination and thin film properties of silicon nitride and amorphous silicon passivated c-Si following ammonia plasma exposure. Applied Physics Letters, 2015, 106, 041607.	3.3	4
54	Proof-of-concept p-type silicon solar cells with molybdenum oxide partial rear contacts. , 2015, , .		3

#	Article	IF	CITATIONS
55	Proof-of-Concept p-Type Silicon Solar Cells With Molybdenum Oxide Local Rear Contacts. IEEE Journal of Photovoltaics, 2015, 5, 1591-1594.	2.5	49
56	Skin care for healthy silicon solar cells. , 2015, , .		57
57	Charge Carrier Separation in Solar Cells. IEEE Journal of Photovoltaics, 2015, 5, 461-469.	2.5	327
58	Phosphorus-diffused polysilicon contacts for solar cells. Solar Energy Materials and Solar Cells, 2015, 142, 75-82.	6.2	147
59	Passivation of c-Si surfaces by ALD tantalum oxide capped with PECVD silicon nitride. Solar Energy Materials and Solar Cells, 2015, 142, 42-46.	6.2	34
60	Tantalum oxide/silicon nitride: A negatively charged surface passivation stack for silicon solar cells. Applied Physics Letters, 2015, 106, .	3.3	26
61	Simple silicon solar cells featuring an a-Si:H enhanced rear MIS contact. Solar Energy Materials and Solar Cells, 2015, 138, 22-25.	6.2	24
62	Demonstration of c-Si Solar Cells With Gallium Oxide Surface Passivation and Laser-Doped Gallium p ⁺ Regions. IEEE Journal of Photovoltaics, 2015, 5, 1586-1590.	2.5	16
63	n- and p-typesilicon Solar Cells with Molybdenum Oxide Hole Contacts. Energy Procedia, 2015, 77, 446-450.	1.8	62
64	Molybdenum oxide MoOx: A versatile hole contact for silicon solar cells. Applied Physics Letters, 2014, 105, .	3.3	279
65	Passivated contacts to n ⁺ and p ⁺ silicon based on amorphous silicon and thin dielectrics. , 2014, , .		10
66	Electrons and holes in solar cells with partial rear contacts. Progress in Photovoltaics: Research and Applications, 2014, 22, 764-774.	8.1	14
67	Towards industrial advanced front-junction n-type silicon solar cells. , 2014, , .		4
68	Empirical determination of the energy band gap narrowing in p+ silicon heavily doped with boron. Journal of Applied Physics, 2014, 116, .	2.5	69
69	The Recombination Parameter JO. Energy Procedia, 2014, 55, 53-62.	1.8	118
70	Development of a self-aligned etch-back process for selectively doped silicon solar cells. , 2014, , .		4
71	Impact of compensation on the boron and oxygen-related degradation of upgraded metallurgical-grade silicon solar cells. Solar Energy Materials and Solar Cells, 2014, 120, 390-395.	6.2	22
72	Effect of boron concentration on recombination at the <i>p</i> -Si–Al2O3 interface. Journal of Applied Physics, 2014, 115, .	2.5	43

#	Article	IF	CITATIONS
73	Reactive ion etched black silicon texturing: A comparative study. , 2014, , .		11
74	Influence of the NH <inf>3</inf> :SiH <inf>4</inf> ratio and surface morphology on the surface passivation of phosphorus-diffused C-Si by PECVD SiN <inf>x</inf> . , 2014, , .		1
75	Surface passivation of crystalline silicon by sputter deposited hydrogenated amorphous silicon. Physica Status Solidi - Rapid Research Letters, 2014, 8, 231-234.	2.4	16
76	Characterization and Diagnosis of Silicon Wafers, Ingots, and Solar Cells. , 2013, , 469-499.		0
77	Empirical determination of the energy band gap narrowing in highly doped n+ silicon. Journal of Applied Physics, 2013, 114, .	2.5	53
78	Low Surface Recombination Velocity by Low-Absorption Silicon Nitride on c-Si. IEEE Journal of Photovoltaics, 2013, 3, 554-559.	2.5	52
79	Misconceptions and Misnomers in Solar Cells. IEEE Journal of Photovoltaics, 2013, 3, 916-923.	2.5	61
80	Process Control of Reactive Sputter Deposition of AlO \$_{x}\$ and Improved Surface Passivation of Crystalline Silicon. IEEE Journal of Photovoltaics, 2013, 3, 183-188.	2.5	20
81	Modelling Silicon Solar Cells with up-to-date Material Parameters. Energy Procedia, 2013, 38, 66-71.	1.8	6
82	Compensation engineering for uniform n-type silicon ingots. Solar Energy Materials and Solar Cells, 2013, 111, 146-152.	6.2	8
83	Passivation of aluminium-n+silicon contacts for solar cells by ultrathin Al2O3and SiO2dielectric layers. Physica Status Solidi - Rapid Research Letters, 2013, 7, 946-949.	2.4	37
84	Enhanced rearâ€side reflection and firingâ€stable surface passivation of silicon solar cells with capping polymer films. Physica Status Solidi - Rapid Research Letters, 2013, 7, 530-533.	2.4	3
85	Physical model of back line-contact front-junction solar cells. Journal of Applied Physics, 2013, 113, 164502.	2.5	26
86	Process control of reactive sputter deposition of AlO <inf>x</inf> and improved surface passivation of crystalline silicon. , 2013, , .		0
87	Low surface recombination velocity by low-absorption silicon nitride on c-Si. , 2013, , .		4
88	Plasma hydrogenated, reactively sputtered aluminium oxide for silicon surface passivation. Physica Status Solidi - Rapid Research Letters, 2013, 7, 619-622.	2.4	15
89	A Contactless Method for Determining the Carrier Mobility Sum in Silicon Wafers. IEEE Journal of Photovoltaics, 2012, 2, 41-46.	2.5	15
90	Process control of reactive sputter deposition of AlO <inf>x</inf> and improved surface passivation of crystalline silicon. , 2012, , .		0

#	Article	IF	CITATIONS
91	Low surface recombination velocity by low-absorption silicon nitride on c-Si. , 2012, , .		5
92	Characterization and Diagnosis of Silicon Wafers, Ingots, and Solar Cells. , 2012, , 1011-1044.		1
93	Improved quantitative description of Auger recombination in crystalline silicon. Physical Review B, 2012, 86, .	3.2	723
94	Modelling silicon characterisation. Energy Procedia, 2011, 8, 94-99.	1.8	28
95	Role of hydrogen in the surface passivation of crystalline silicon by sputtered aluminum oxide. Progress in Photovoltaics: Research and Applications, 2011, 19, 320-325.	8.1	21
96	Recombination in compensated crystalline silicon for solar cells. Journal of Applied Physics, 2011, 109, 043704-043704-8.	2.5	28
97	Thermal activation energy for the passivation of the n-type crystalline silicon surface by hydrogenated amorphous silicon. Applied Physics Letters, 2009, 94, .	3.3	40
98	Effective surface passivation of crystalline silicon by rf sputtered aluminum oxide. Physica Status Solidi - Rapid Research Letters, 2009, 3, 160-162.	2.4	134
99	The paradox of compensated silicon. Optoelectronic and Microelectronic Materials and Devices (COMMAD), Conference on, 2008, , .	0.0	8
100	Limitations of a simplified dangling bond recombination model for a-Si:H. Journal of Applied Physics, 2008, 104, .	2.5	10
101	FTIR Analysis of Microwave-Excited PECVD Silicon Nitride Layers. , 2006, , .		6
102	Capturing the spectral response of solar cells with a quasi-steady-state, large-signal technique. Progress in Photovoltaics: Research and Applications, 2006, 14, 203-212.	8.1	9
103	Unveiling the Injection-Dependence of the Diffusion Length Via the Spectral Response of the Voltage of Silicon Solar Cells. , 2006, , .		1
104	Recombination in n- and p-Type Silicon Emitters Contaminated with Iron. , 2006, , .		2
105	Characterisation and diagnosis of silicon wafers and devices. , 2005, , 163-188.		3
106	Behaviour of Natural and Implanted Iron during Annealing of Multicrystalline Silicon Wafers. Solid State Phenomena, 2005, 108-109, 519-524.	0.3	3
107	Open-circuit voltage quantum efficiency technique for defect spectroscopy in semiconductors. Applied Physics Letters, 2005, 87, 104102.	3.3	0
108	Generalized models of the spectral response of the voltage for the extraction of recombination parameters in silicon devices. Journal of Applied Physics, 2005, 98, 083708.	2.5	6

#	Article	IF	CITATIONS
109	Transition-metal profiles in a multicrystalline silicon ingot. Journal of Applied Physics, 2005, 97, 033523.	2.5	182
110	The Role of Silicon Interstitials in the Formation of Boron-Oxygen Defects in Crystalline Silicon. Solid State Phenomena, 2005, 108-109, 497-502.	0.3	10
111	Measuring and interpreting the lifetime of silicon wafers. Solar Energy, 2004, 76, 255-262.	6.1	255
112	Limiting efficiency of crystalline silicon solar cells due to Coulomb-enhanced Auger recombination. Progress in Photovoltaics: Research and Applications, 2003, 11, 97-104.	8.1	138
113	Validity of simplified Shockley-Read-Hall statistics for modeling carrier lifetimes in crystalline silicon. Physical Review B, 2003, 67, .	3.2	81
114	Characterisation and Diagnosis of Silicon Wafers and Devices. , 2003, , 227-252.		1
115	Generalized analysis of quasi-steady-state and transient decay open circuit voltage measurements. Journal of Applied Physics, 2002, 91, 399.	2.5	133
116	Recombination at the interface between silicon and stoichiometric plasma silicon nitride. Semiconductor Science and Technology, 2002, 17, 166-172.	2.0	111
117	General parameterization of Auger recombination in crystalline silicon. Journal of Applied Physics, 2002, 91, 2473-2480.	2.5	399
118	Numerical modeling of highly doped Si:P emitters based on Fermi–Dirac statistics and self-consistent material parameters. Journal of Applied Physics, 2002, 92, 3187-3197.	2.5	154
119	Very low bulk and surface recombination in oxidized silicon wafers. Semiconductor Science and Technology, 2002, 17, 35-38.	2.0	238
120	Millisecond minority carrier lifetimes in n-type multicrystalline silicon. Applied Physics Letters, 2002, 81, 4952-4954.	3.3	76
121	A contactless photoconductance technique to evaluate the quantum efficiency of solar cell emitters. Solar Energy Materials and Solar Cells, 2002, 71, 295-312.	6.2	29
122	Surface passivation of silicon solar cells using plasma-enhanced chemical-vapour-deposited SiN films and thin thermal SiO2/plasma SiN stacks. Semiconductor Science and Technology, 2001, 16, 164-170.	2.0	210
123	On the use of a bias-light correction for trapping effects in photoconductance-based lifetime measurements of silicon. Journal of Applied Physics, 2001, 89, 2772-2778.	2.5	67
124	Capture cross sections of the acceptor level of iron–boron pairs in p-type silicon by injection-level dependent lifetime measurements. Journal of Applied Physics, 2001, 89, 7932-7939.	2.5	75
125	Understanding carrier trapping in multicrystalline silicon. Solar Energy Materials and Solar Cells, 2001, 65, 509-516.	6.2	35
126	Impact of light-induced recombination centres on the current-voltage characteristic of czochralski silicon solar cells. Progress in Photovoltaics: Research and Applications, 2001, 9, 249-255.	8.1	25

#	Article	IF	CITATIONS
127	Comment on "Mechanisms for the anomalous dependence of carrier lifetime on injection level and photoconductance on light intensity―[J. Appl. Phys.89, 332 (2001)]. Journal of Applied Physics, 2001, 90, 2621-2622.	2.5	1
128	Reduced fill factors in multicrystalline silicon solar cells due to injection-level dependent bulk recombination lifetimes. Progress in Photovoltaics: Research and Applications, 2000, 8, 363-375.	8.1	85
129	Comparison of the open circuit voltage of simplified PERC cells passivated with PECVD silicon nitride and thermal silicon oxide. Progress in Photovoltaics: Research and Applications, 2000, 8, 529-536.	8.1	22
130	Co-optimisation of the emitter region and the metal grid of silicon solar cells. Progress in Photovoltaics: Research and Applications, 2000, 8, 603-616.	8.1	52
131	Reduced fill factors in multicrystalline silicon solar cells due to injection-level dependent bulk recombination lifetimes. , 2000, 8, 363.		1
132	Boron-related minority-carrier trapping centers in p-type silicon. Applied Physics Letters, 1999, 75, 1571-1573.	3.3	35
133	The effect of emitter recombination on the effective lifetime of silicon wafers. Solar Energy Materials and Solar Cells, 1999, 57, 277-290.	6.2	107
134	Electronic properties of light-induced recombination centers in boron-doped Czochralski silicon. Journal of Applied Physics, 1999, 86, 3175-3180.	2.5	187
135	High minority carrier lifetime in phosphorus-gettered multicrystalline silicon. Applied Physics Letters, 1997, 70, 1017-1019.	3.3	44
136	Prediction of the open-circuit voltage of solar cells from the steady-state photoconductance. Progress in Photovoltaics: Research and Applications, 1997, 5, 79-90.	8.1	122
137	Surface recombination velocity of highly dopednâ€ŧype silicon. Journal of Applied Physics, 1996, 80, 3370-3375.	2.5	200
138	Contactless determination of current–voltage characteristics and minority arrier lifetimes in semiconductors from quasiâ€steadyâ€state photoconductance data. Applied Physics Letters, 1996, 69, 2510-2512.	3.3	1,383
139	Influence of the dopant density profile on minority-carrier current in shallow, heavily doped emitters of silicon bipolar devices. Solid-State Electronics, 1985, 28, 247-254.	1.4	14